

## Size Dependence of Transport Property in $Ce_{1-x}Zr_xO_2$ ( $x = 0.2-0.8$ ) Solid Solution

M. Kalpana<sup>1</sup> and B. Nalini<sup>2\*</sup>

<sup>1</sup>*Department of Physics, Karunya University, Coimbatore-641 114,  
Tamilnadu, India*

<sup>2</sup>*Centre for Nanotechnology, Karunya University,  
Coimbatore-641 114, Tamilnadu, India*

*\*Corresponding Author E-mail: jyothsnalalin99@gmail.com*

### Abstract

Nanosized ceria doped zirconia solid solution is the material of attraction for the intermediate temperature solid oxide fuel cell. A systematic study has been carried out on  $Ce_{1-x}Zr_xO_2$  with the composition of  $x = 0.2, 0.4, 0.5, 0.6, 0.8$  by co-precipitation method. Structural elucidations were made through XRD to ascertain the attainment of phase and nano-crystallite size. The electrical properties of  $Ce_{1-x}Zr_xO_2$ , employing ac impedance spectroscopy, show that the size dependence brings change in transport property. The reduction in size brings higher grain boundary impedance which is a contrary behavior observed in nanosized particles.

**Keywords:** IT-SOFC, Nanocrystalline, Cerium/Zirconium solid solution, Impedance analysis.

### Introduction

A major technological breakthrough in developing intermediate temperature solid oxide fuel cells (SOFC) is employing Ceria based electrolytes in order to reduce the cost and increase the fuel cell lifetime. Nevertheless, decrease in the operating temperature leads to losses in cell performance mainly due to the ohmic drop through the electrolyte. [1] Yttria stabilized zirconia (YSZ) is the most commonly used electrolyte but its ionic conductivity falls from  $0.1 \text{ S.cm}^{-1}$  at 1273 K to  $0.02 \text{ S.cm}^{-1}$  at 1073 K [2] on cyclic operation. However at lower temperatures, the ionic conductivity of YSZ is much lower than that of ceria-based electrolytes. Horita et al., [3] have

reported ceria-zirconia-ceria sandwich structured composite film electrolytes to possess high ionic conductivity compared to YSZ and have reported two orders of magnitude increase from bulk to thin film. The need of an alternative electrolyte which has higher ionic conductivity than YSZ and more stable for thermal operation has resulted in cerium doped zirconia.

At this juncture, the nanocrystalline materials have superior powder properties such as large surface area and better sinter ability etc. The nanosized electroceramic particles are expected to improve the ionic conductivity making the system more suitable as an electrolyte with better thermal expansion. But very few literatures are available for the preparation of nanosized  $Ce_{1-x}Zr_xO_2$  from the low temperature method.

Many methods have been employed for the preparation of nanosized  $CeO_2-ZrO_2$ . In this earliest work, the precipitation of Zirconia-based solid solutions involved high temperature (900-1500°C) techniques, resulting in unrestrained grain growth, thus low surface area materials, segregation of dopant and possible loss of stoichiometry due to volatilization of a reactant at high temperatures.[4] Hori et al.[5] have prepared  $CeO_2-ZrO_2$  employing  $(NH_4)_2Ce(NO_3)_6$  and  $ZrO(NO_3)_2$  as precursors by calcinations at 500°C, which was claimed as the lowest temperature used so far obtain  $CeO_2-ZrO_2$  solid solution. But they have reported the particle sizes of the samples aged at 1000°C in the range of 19-73nm determined by XRD. Letichevsky et al. [6] have prepared  $CeO_2-ZrO_2$  solid solution according to the procedure followed by Hori et al. [5] and also they have reported the more relevant experimental parameters such as pH, aging, drying, calcination condition and Ce precursor. It has been found that the particle size is in range of 39nm - 44nm from XRD. Zhang et al. [7] have reported the synthesis of  $Ce_{0.6}Zr_{0.4}O_2$  solid solutions by different methods. It has been found that the co-precipitated powders calcined at 500°C having the particle diameter of 45.99µm. Grover et al.[8] have prepared nanocrystalline ceria-doped-zirconia powder ( $Zr_{0.80}Ce_{0.20}O_{0.20}$ ) by combustion technique which provides more results for oxidation and wide particle size distribution. Potdar et al. [9] have prepared nanosized  $Ce_{0.75}Zr_{0.25}O_{0.20}$  porous powders via an auto ignition process.

The electrical properties of  $Ce_{1-x}Zr_xO_2$  solid solutions are inadequately investigated. It is believed that these solid solutions possess electronic-ionic conductivity.[10] However, it remains unclear whether their ionic conductivity depends on the crystal size.

The present work focuses on the preparation of  $Ce_{1-x}Zr_xO_2$  ( $x = 0.2-0.8$ ) by co-precipitation method which is a simple route with optimized process for attainment of nanosize and the zirconia was doped with  $CeO_2$  to see whether the grain conductivity increases and to investigate the factors controlling the grain conductivity of ceria. Here, we report the effect of Zr addition on structural and especially the effect of grain size on the electrical conductivity of Zr doped  $CeO_2$  at room temperature. The structural properties, morphology of the powders were studied by XRD and SEM respectively. The electrical conductivity and the dielectric properties of the calcined powders have been investigated by AC Impedance Analyzer.

### Experimental Details

The  $Ce_{1-x}Zr_xO_2$  ( $x = 0.2, 0.4, 0.5, 0.6, 0.8$ ) solid solutions were prepared at five different composition by co-precipitation method according to the procedure followed by Letichevsky et al.,[6] with the optimized parameters such as pH control, aging of solution. Basically, a solution of  $NH_4OH$  was quickly added to aqueous solution of ammonium cerium (IV) nitrate and zirconium nitrate in the desired Ce: Zr (wt %) ratio under vigorous stirring. The pH value was adjusted for 12 using  $NH_4OH$  solution. After 48 h of aging at room temperature, a pure precipitate was filtered and washed with deionized water repeatedly until no pH change to ensure the complete removal of the base. Then the precipitate was dried under ventilated conditions at room temperature overnight. Finally, the yellow precipitate was calcined in air at  $500^\circ C$  for 2 h in a muffle furnace. The sintering temperature was set below  $500^\circ C$  without allowing the grain growth thus preserving the size of the particles as precipitated. Since the non-calcined powders resulted in poor crystallinity, the powders were calcined at  $500^\circ C$ .

X-ray diffraction analysis was performed by Shimadzu-Model XRD-6000 diffractometer, operating voltage of 40KV and current of 30mA, using Cu-K $\alpha$  radiation ( $1.5406\text{\AA}$ ) for an angular range of  $10^\circ$ - $100^\circ$ , with increments of  $0.1^\circ$  and counting time of 1.2 s per step. Scanning Electron Microscope (SEM Model-JEOL.JSM-6390) was used for microstructural analysis such as size, shape and morphology of the calcined powder and its agglomerates. For electrical conductivity measurements the calcined powders were ground in a mortar and then pressed into pellets with 10mm diameter via hydraulic pressing under a pressure of 200MPa. The impedance analyses were performed using a HP 4284a LCR meter over the frequency range 20 Hz - 1MHz at room temperature for all the compositions using the silver electrodes.

## Results and Discussion

### X-ray diffraction (XRD)

Fig.1 shows the broad XRD peaks of  $Ce_{1-x}Zr_xO_2$  ( $x=0.2-0.8$ ) powders calcined at  $500^\circ C$ . According to Scherrer equation Eq. (1)

$$D = \frac{0.9 \lambda}{\beta \cos \theta} \quad (1)$$

where D is the crystallite size,  $\lambda$  the wavelength of the radiation ( $1.5405\text{\AA}$  for Cu-K $\alpha$  radiation),  $\beta$  the full width at half maximum of the peak, and  $\theta$  is the peak position. The calculated average crystallite size of the  $Ce_{1-x}Zr_xO_2$  powder was 1-10nm after being calcined at  $500^\circ C$  for 1h. The XRD pattern has four main reflections corresponding to cubic structure namely [111], [200], [220] and [311] planes and corresponding to tetragonal structure namely [101], [110], [112] and [211] planes [JCPDS card:28-0271,38-1439,38-1436,80-0785] as indicated in the Figure 1.

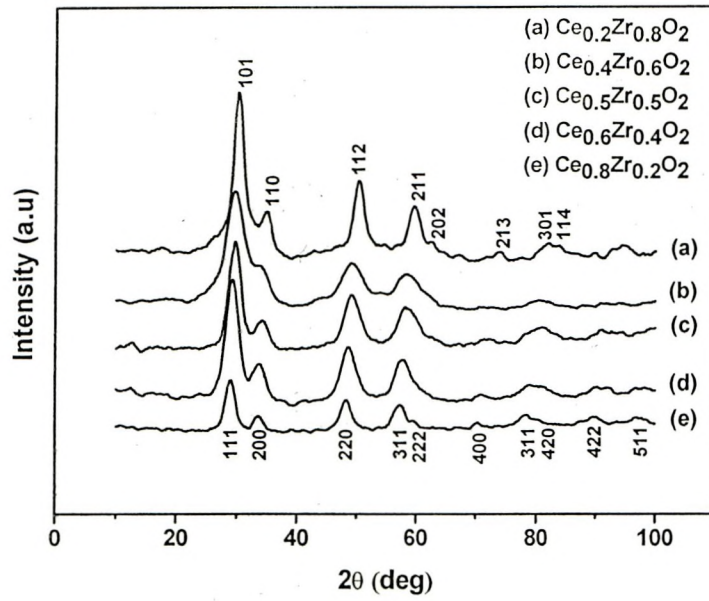


Figure 1: XRD pattern of  $Ce_{1-x}Zr_xO_2$  ( $x = 0.2, 0.4, 0.5, 0.6, 0.8$ )

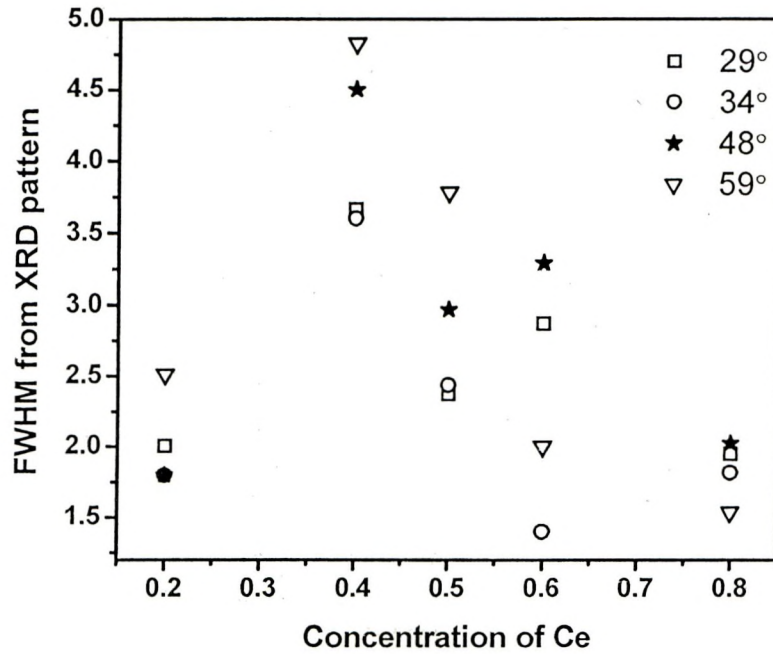


Figure 2: FWHM values from XRD pattern with various concentration of Ce (0.2, 0.4, 0.5, 0.6, 0.8)

**Table 1:** Calculated lattice parameters for  $Ce_{1-x}Zr_xO_2$  ( $x = 0.2, 0.4, 0.5, 0.6, 0.8$ )

Sample name	Crystal structure	Lattice constant		Particle size from XRD in nm
		A	C	
$Ce_{0.2}Zr_{0.8}O_2$	Tetragonal	5.201	3.601	2-8
$Ce_{0.4}Zr_{0.6}O_2$	Tetragonal	5.252	3.653	1-4
$Ce_{0.5}Zr_{0.5}O_2$	Tetragonal	5.310	3.660	2-10
$Ce_{0.6}Zr_{0.4}O_2$	Cubic	5.287	--	2-7
$Ce_{0.8}Zr_{0.2}O_2$	Cubic	5.337	--	4-10

The lattice parameters were calculated and are shown in Table.1. It is seen from the Figure 1 that the increasing concentration of Ce in  $ZrO_2$  lattice results in alteration of atomic arrangement resulting in a phase transition from tetragonal to cubic due to the substitution of Ce in the tetrahedral sites. [11] It is to be noted here that the composition reported in the reference stated above is a non-stoichiometric one where there is ample of chances for impurity driven activities concerned. In the ratio of  $Ce_{0.5}Zr_{0.5}O_2$ , a mixed phase of both cubic and tetragonal are found. After which the phase has no traces of the cubic phase. It can be evident from the phase diagram of zirconia-ceria system, it is shown that there exists an expanded two-phase region around the equimolar composition of the system [12, 13]. Accordingly, the lattice parameter is found to decrease linearly from 5.337 Å to 5.201 Å with increase in  $ZrO_2$  content followed the Vegard's law except for  $x = 0.5$ . Ranga Rao et al. [14] have prepared the  $CeO_2$ - $ZrO_2$  solid solutions by combustion method. They have reported that the lattice parameter is linearly decreased from 5.44Å-5.20Å with increase of  $ZrO_2$  content. Figure.2. shows the variation of the peak broadening (FWHM) for the corresponding  $2\theta$  values from XRD of each concentration of Ce. The particle size effects can be observed through the peak broadening. The peak broadening is obviously seen from the XRD spectra indicating that smaller crystallite size have resulted in this preparation.

#### Scanning Electron Microscope (SEM)

The Fig. 3(a-e) shows the morphology of  $Ce_{1-x}Zr_xO_2$  ( $x = 0.2-0.8$ ) powders calcined at 500°C. From the SEM analysis, the particle size of the powders is in the range of 80-125nm for  $Ce_{0.2}Zr_{0.8}O_2$ , 50-100nm for  $Ce_{0.5}Zr_{0.5}O_2$  and 80-150nm for  $Ce_{0.8}Zr_{0.2}O_2$ . In  $Ce_{0.4}Zr_{0.6}O_2$  and  $Ce_{0.6}Zr_{0.4}O_2$  composition, the agglomeration could not be prevented by any of the employed processes. Hence it is suggested that specific processes need to be employed for the unfoliation of the agglomerated particles which is not presented in this paper.

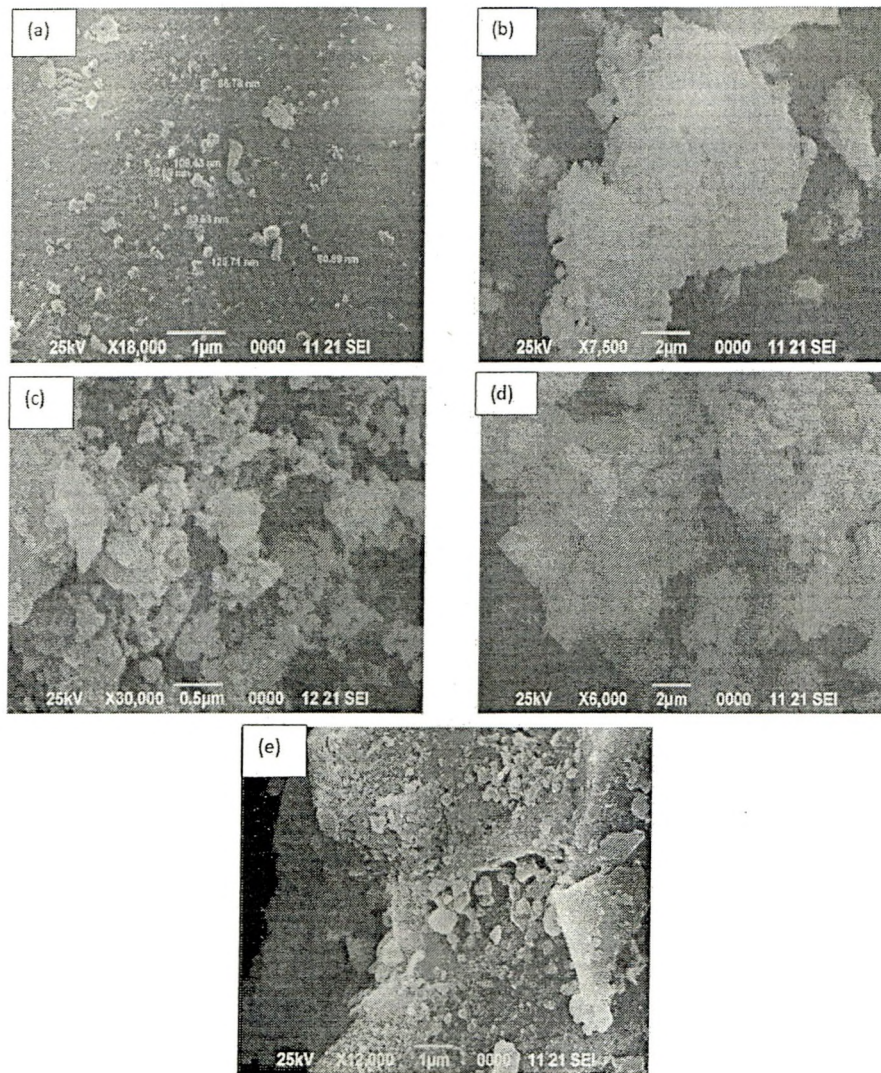


**Figure 3:** (a-e).SEM images of  $Ce_{1-x}Zr_xO_2$  powders calcined at 500°C. (a)  $x = 0.2$ , (b)  $x = 0.4$ , (c)  $x = 0.5$ , (d)  $x = 0.6$ , (e)  $x = 0.8$

It is found in the literature, [9] that nanosized  $Ce_{0.75}Zr_{0.25}O_2$  powders were prepared via an auto ignition method which resulted in severe agglomeration. It is to be noted that the process of co-precipitation have yielded better isolated particles in this present work for the same composition.

#### Electrical conductivity

Impedance spectroscopy helps to resolve the grain and grain-boundary effects as well as the electrode kinetic properties. The response of these processes manifests as semi-circles in a Nyquist plot. [15] Usually the high frequency semicircle is mainly

contributed by bulk, while the low frequency semicircle is by grain boundary. With the increase of frequency, the intercept on the real axis, viz  $\text{Re}(Z)$  decreases. Typical impedance spectra of pelletized samples of  $\text{Ce}_{1-x}\text{Zr}_x\text{O}_2$  ( $x=0.2-0.8$ ) calcined at  $500^\circ\text{C}$  are shown in Fig.4. Each semi-circle response on the Nyquist plot was fitted with a simple circuit using the Z-View software. The equivalent circuit includes a series resistance ( $R_s$ ) with a Constant Phase Element (CPE) at room temperature.

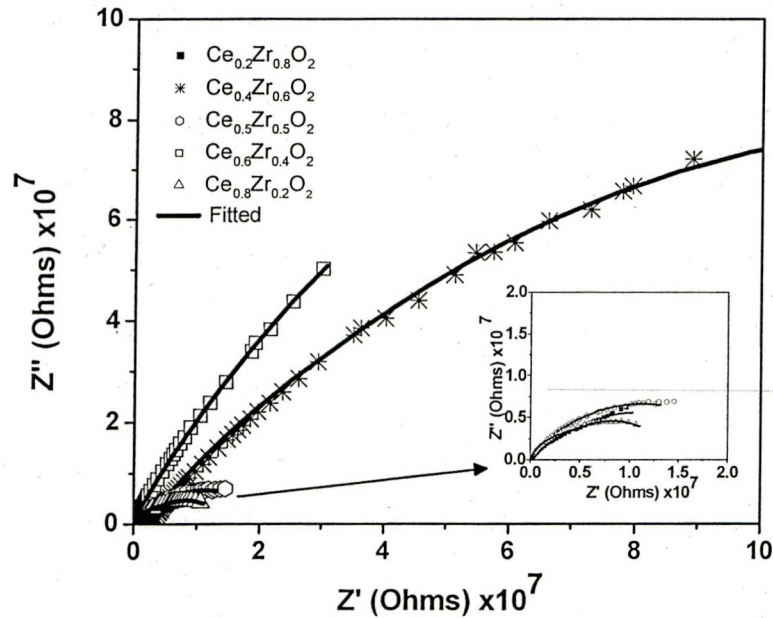


**Figure 4:** Impedance spectrum with fitting curve of  $\text{Ce}_{1-x}\text{Zr}_x\text{O}_2$  ( $x = 0.2, 0.4, 0.5, 0.6, 0.8$ ) at room temperature

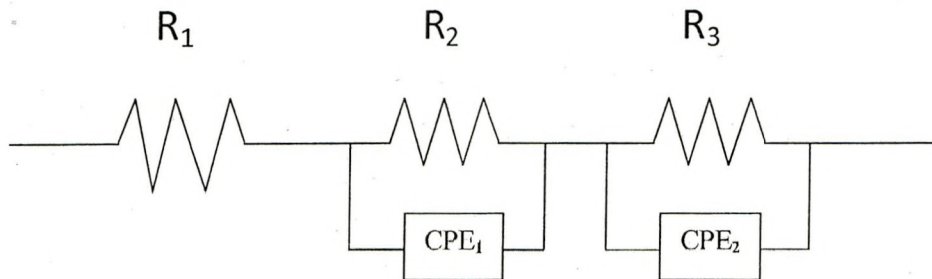


**Figure 5:** Equivalent circuit for  $\text{Ce}_{1-x}\text{Zr}_x\text{O}_2$

**Table 2:** Equivalent circuit values for  $Ce_{1-x}Zr_xO_2$ 

Sample name	$R_s$	$R_1$	$R_2$	CPE 1		CPE2	
				T	P	T	P
$Ce_{0.2}Zr_{0.8}O_2$	10	1.84E+06	1.90E+07	1.34E-10	0.7721	4.27E-10	0.6743
$Ce_{0.4}Zr_{0.6}O_2$	-	2.47E+06	8.55E+07	4.67E-11	0.6512	8.68E-12	0.9900
$Ce_{0.5}Zr_{0.5}O_2$	10	2.15E+06	1.93E+07	1.22E-10	0.7438	2.13E-10	0.7263
$Ce_{0.6}Zr_{0.4}O_2$	10	3.14E+06	3.55E+08	9.29E-11	0.8260	2.27E-11	0.7721
$Ce_{0.8}Zr_{0.2}O_2$	-	4.77E+06	9.42E+06	8.29E-11	0.8200	1.52E-10	0.8852

The values acquired using the theoretical fit to the equivalent circuits are shown in Table.2. Fig.4 and 5 shows the fitted graph and the equivalent circuit of the sample  $Ce_{1-x}Zr_xO_2$ . The equivalent circuit suggests that the material contains grain and grain boundary resistances by two CPE elements in parallel to resistances respectively. The total electrical conductivity of all the composition were calculated and found to be approximately same conductivity in the range of  $8.57 \times 10^{-6} - 28.45 \times 10^{-6}$  S/m. The calculated conductivity values are shown in Table.3. Xu et al. [16] have reported the conductivity of cubic  $Ce_{0.5}Zr_{0.5}O_2$ . It can be found that the conductivity enhances gradually with temperature increasing ( $\sigma = 1.2 \times 10^{-5}$  S/cm at 823 K and  $\sigma = 2.1 \times 10^{-3}$  S/cm at 1123 K), which is the same as that of pure CeO<sub>2</sub> at 823 K, but smaller than that of doped-zirconia at 1123 K. Chiodelli et al. [17] have reported the electrical properties of ZrO<sub>2</sub>-CeO<sub>2</sub> solid at the temperature range of 200-1000°C. 900°C, pure CeO<sub>2</sub>, exhibits a conductivity  $\sigma = 1.9 \times 10^{-4} \Omega\text{cm}^{-1}$ , whereas in the 80 mol% CeO<sub>2</sub>, solid solution the conductivity is  $\sigma = 1 \times 10^{-2} \Omega\text{cm}^{-1}$ . Bin Zhu et al. [18] have reported the electrical properties of the ZrO<sub>2</sub>-CeO<sub>2</sub> at Intermediate temperatures. The thin films have very different properties, e.g. they are less affected by reduced atmospheres and are highly conductive, two orders of magnitude higher than the bulk materials ( $10^{-2}$  S/cm of the films compared to  $10^{-4}$  S/cm of the bulk samples at 600°C. Takahisa et al. [19] have reported the review works on Nanocrystals (NC) of zirconia and ceria-based solid electrolytes. According to the electrical conductivity studies of the YSZ microcrystallines, the total conductivity decreased with decreasing grain size, because the grain boundary conductivity decreased with decreasing grain size. In contrast to the microcrystalline case, the enhanced conductivity upon decreasing the grain size was observed for the YSZ NCs, whose grain size was less than 100 nm. Lee et al. [20] have reported the electrical conductivity and defect structure of CeO<sub>2</sub>-ZrO<sub>2</sub> mixed oxide. The electrical conductivity increased as CeO<sub>2</sub> concentration increased and maximum value of electrical conductivity was found at 90m/oCeO<sub>2</sub> system and then decreased for pure CeO<sub>2</sub>. The ionic conduction prevailing in the ZrO<sub>2</sub> rich phase due to the increase of ionic defect concentration via homovalent doping effect. The enhancement of n-type electronic conductivity was observed in intermediate and CeO<sub>2</sub> rich phase compared with pure CeO<sub>2</sub>, which originated either from homovalent doping effect of increase of electronic mobility due to the change of transport mechanism.

**Table 3:** Calculated conductivity values for  $Ce_{1-x}Zr_xO_2$  ( $x = 0.2, 0.4, 0.5, 0.6, 0.8$ )

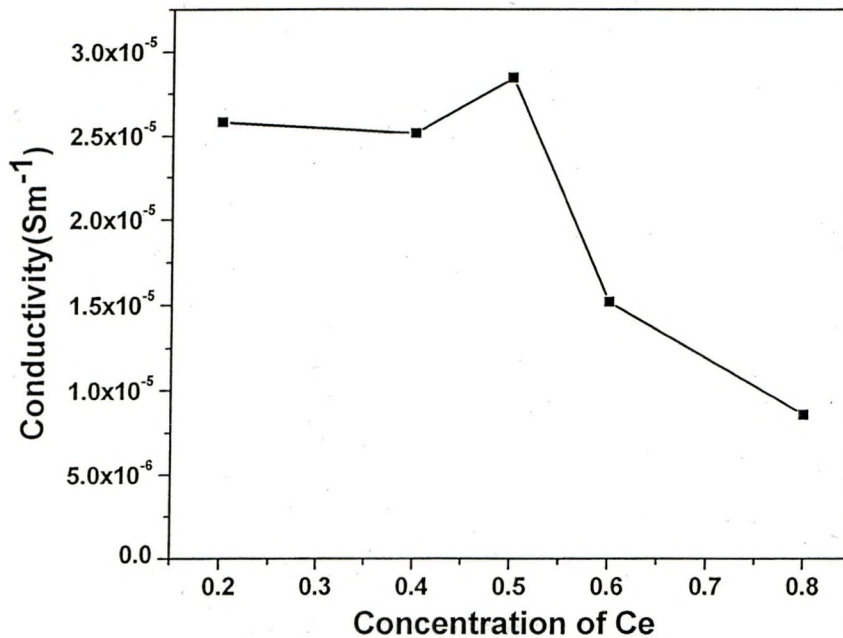
Sample name	Thickness in meter	Area in meter <sup>2</sup>	Grain Resistance	Grain Conductivity	Grain Boundary Resistance	Grain Boundary Conductivity	Total conductivity in S/m
$Ce_{0.2}Zr_{0.8}O_2$	3.41E-03	7.85E-05	1.84E+06	2.3550E-05	1.90E+07	2.2819E-06	2.5832E-05
$Ce_{0.4}Zr_{0.6}O_2$	4.21E-03	7.85E-05	2.41E+06	2.2235E-05	1.84E+07	2.9098E-06	2.5145E-05
$Ce_{0.5}Zr_{0.5}O_2$	4.32E-03	7.85E-05	2.15E+06	2.5601E-05	1.93E+07	2.8519E-06	2.8453E-05
$Ce_{0.6}Zr_{0.4}O_2$	3.71E-03	7.85E-05	3.14E+06	1.5053E-05	3.55E+08	1.3331E-07	1.5186E-05
$Ce_{0.8}Zr_{0.2}O_2$	2.13E-03	7.85E-05	4.77E+06	5.6928E-06	9.42E+06	2.8810E-06	8.5738E-06

### Concentration dependence of ionic Conductivity

The ionic conductivity values of the electrolytes are calculated by using the equation:

$$\sigma = l / R_b A \quad (2)$$

where  $l$  and  $A$  are the thickness and known area of the electrolyte and  $R_b$  is the bulk resistance of the electrolyte. Fig.6 shows the variation of the total conductivity of  $Ce_{1-x}Zr_xO_2$  with respect to the concentration of Ce. It has been found that the total conductivity decreases as the concentration of Ce increases.

**Figure 6:** Ce Concentration dependence of Conductivity

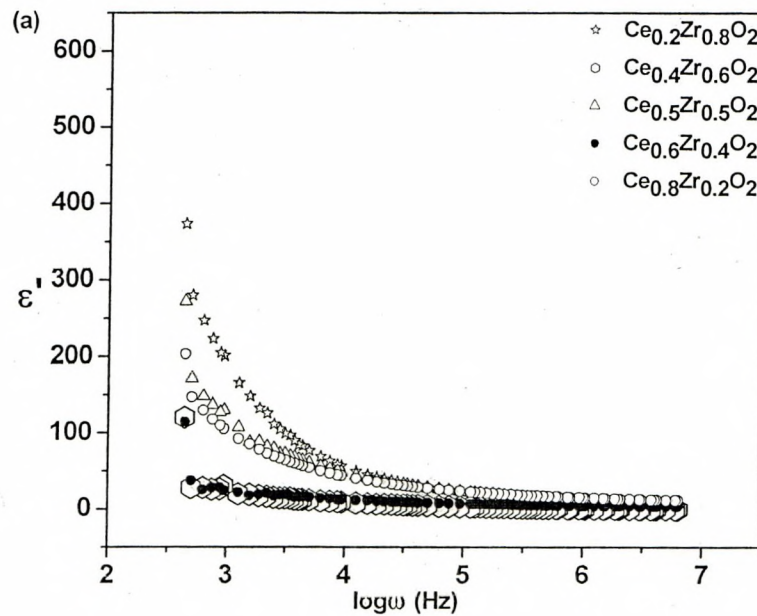
However an increase in conductivity is observed only for  $\text{Ce}_{0.5}\text{Zr}_{0.5}\text{O}_2$  sample. This may be due to the formation of ion clusters, thus decreasing the scattering sites for the mobile charge carriers. The "brick-layer" model calculations suggest that grain interior and grain boundary arcs will be virtually indistinguishable at the small grain sizes involved in the present work.[21]

### Dielectric analysis

The dielectric response is generally described by the complex permittivity,

$$\epsilon^* = \epsilon'(\omega) - j\epsilon''(\omega) \quad (3)$$

where real  $\epsilon'(\omega)$  and imaginary  $\epsilon''(\omega)$  components are the storage and loss of energy in each cycle of the applied electric field. [22] Figure 7(a and b) represents the frequency dependence of  $\epsilon'(\omega)$  and  $\epsilon''(\omega)$  for Ce doped Zr with different concentrations at room temperature. From the figures, it is clear that the values of  $\epsilon'(\omega)$  are very high at low frequency. Such high value of dielectric permittivity at low frequencies has been explained by the presence of space charge effects, which is contributed by the accumulation of charge carriers near the electrodes. At higher frequencies,  $\epsilon'(\omega)$  has been found to be relatively constant with frequency.



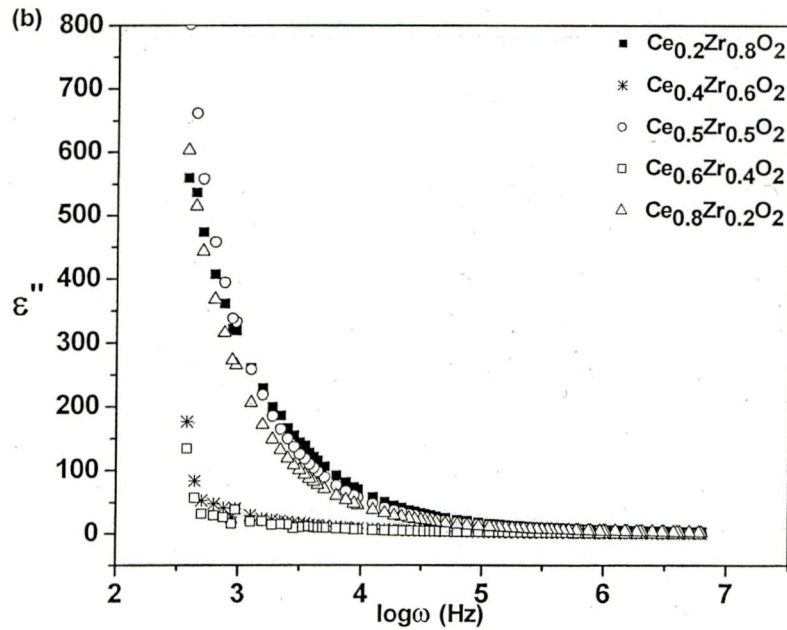


**Figure 7:** Frequency dependence of (a) real part  $\epsilon'(\omega)$  and (b) imaginary part  $\epsilon''(\omega)$  of dielectric permittivity for  $\text{Ce}_{1-x}\text{Zr}_x\text{O}_2$  ( $x = 0.2, 0.4, 0.5, 0.6, 0.8$ )

This is because periodic reversal of the field takes place so rapidly that the charge carriers will hardly be able to orient themselves in the field direction resulting in the decrease in dielectric constant. The large value of  $\epsilon''(\omega)$  is also due to the motion of free charge carrier within the material.[23] According to the theory, the dielectric behavior of the nanostructured material is mainly due to different types of polarizations present in the material.[24] The nanostructured material possesses enormous number of interfaces, and the large number of defects present in these interfaces can cause a change of positive or negative space charge distribution. When an electric field is applied these space charges move and are trapped by these defects resulting in the formation of dipole moments. This is called space charge polarization. Interface in the nanostructured materials possesses many oxygen ion vacancies, which are equivalent to positive charges giving dipole moments. Exposed to an electric field, these dipoles will rotate, giving a resultant dipole moment in the direction of the applied field. This is called rotation direction polarization.[25] Thus the high value of dielectric constant at low frequencies is primarily due to the space charge polarization and rotation direction polarization.[26] It can be seen from the values of dielectric constant decreases with increasing concentration of Ce. On the other hand, at high frequencies the non-Debye behavior is observed, which indicates the possible cation motion through the conduction pathways. [27, 28]

## Conclusion

$Ce_{1-x}Zr_xO_2$  solid solutions have been synthesized by co-precipitation method. The XRD results show the crystalline nature of the substance. The XRD patterns of  $Ce_{1-x}Zr_xO_2$  ( $x=0.2-0.8$ ) shows the cubic phase. The SEM analysis reveals a range of particle size between 50-150nm for all the powders and  $Ce_{0.4}Zr_{0.6}O_2$  and  $Ce_{0.6}Zr_{0.4}O_2$  are well agglomerated to a size of 0.5 – 2  $\mu m$ . The impedance confirmed the contribution of grain and grain boundary resistances and the electrical conductivity of the samples ranging between  $8.57 \times 10^{-6}$  –  $28.45 \times 10^{-6} S/m$ . The regular understanding of stating that the nanosized particles would bring higher conduction is true however the grain boundary resistance contribution is more which indicates that the ionic conduction when employed in fuel cell applications would be still limited due to this factor and also the phase change with oxidation.

## References

- [1] Gourba, E., Ringuede, A., Cassir, M., Billard, A., Paivanisaari, J., Niinisto, J., Putkonen, M., and Niinisto, L., 2003, "Characterization of thin films of ceria-based electrolytes for Intermediate Temperature - Solid oxide fuel cells (IT-SOFC)," *Ionics.*, 9, pp. 15-20.
- [2] Will, J., Mitterdorfer, A., Kleinlogel, C., Perednis, D., and Gauckler, L.R., 2000, "Fabrication of thin electrolytes for second-generation solid oxide fuel cells," *Solid State Ionics.*, 131, pp. 79-96.
- [3] Teruhisa Horita, Natsuko Sakai, Harumi Yokokawa, Masayuki Dokiya, Tatsuya Kawada, Jan Van Herle, and Kazutaka Sasaki, 1997, "Ceria-Zirconia Composite Electrolyte for Solid Oxide Fuel Cells," *Journal of Electroceramics.*, 1:2, pp. 155-164.
- [4] Yashima, M., Morimoto, K., Ishizawa, N., and Yoshimura, M., 1993, "Zirconia-Ceria solid solution synthesis and the temperature-time-transformation diagram for the 1:1 composition," *J.Am.Ceram.Soc.*, 76, pp. 1745-1750.
- [5] Carla E. Hori, Haryani Permana, Simon Ng, K.Y., Alan Brenner, Karren More, Kenneth M. Rahmoeller, and David Belton, 1998, "Thermal stability of oxygen storage properties in a mixed  $CeO_2$ - $ZrO_2$  system," *Journal of Applied Catalysis B: Environmental.*, 16, pp. 105-117.
- [6] Sonia Letichevsky, Claudio A. Tellez, Roberto R. de Avillez, Maria Isabel P. da Silva, Marco A. Fraga, and Lucia G. Appel, 2005, "Obtaining  $CeO_2$ - $ZrO_2$  mixed oxides by co precipitation: role of preparation conditions," *Applied Catalysis B: Environmental.*, 58, pp. 203-210.
- [7] Zhaoliang Zhang, Yexin Zhang, Zonggang Mu, Pengfei Yu, Xianzhi Ni, Shilong Wang, Lisheng Zheng, 2007, "Synthesis and catalytic properties of  $Ce_{0.6}Zr_{0.4}O_2$  solid solutions in the oxidation of soluble organic fraction from diesel engines," *Applied Catalysis B: Environmental.*, 76, pp. 335-347.

- [8] Grover, V., Chavan, S.V., Sastry, P.U., and Tyagi, A.K., 2008, "Combustion synthesis of nanocrystalline  $Zr_{0.80}Ce_{0.20}O_2$ : Detailed investigations of the powder properties," *Journal of Alloys and Compounds*, 457, pp. 498-505.
- [9] Potdar, H.S., Deshpande, S.B., Kholam, Y.B., Deshpande, A.S., and Date, S.K., 2003, "Synthesis of  $Ce_{0.75}Zr_{0.25}O_2$  porous powders via an autoignition:glycine nitrate process," *Materials Letters.*, 57, pp. 1066-1071.
- [10] Glushkova, V.B., Popov, V.P., Tikhonov, P.A. Podzorova, L.I., and Il'icheva, A. A., 2006, "Electric Transport Properties and the Size Effect in  $ZrO_2$ -Based Ceramic Materials," *Glass Physics and Chemistry.*, 32(5), pp. 587-590,
- [11] James B. Thomson, Robert Armstrong, A., and Peter G. Bruce., 1996, "A New Class of Pyrochlore Solid Solution Formed by Chemical Intercalation of Oxygen," *J. Am. Chem. Soc.*, 118 (45), pp 11129-11133.
- [12] Yashima, M., Takashina, H., Kakihana, M., and Yoshimura, M., 1994, "Low-temperature phase equilibria by the flux method and the metastable-stable phase diagram in the  $ZrO_2$ - $CeO_2$  system," *J.Am.Ceram.Soc.*, 77, pp. 1869-1874.
- [13] Yoshimura, M., Tani, E., and Somiya, S., 1981, "The confirmation of phase equilibria in the system  $ZrO_2$ - $CeO_2$  below 1400°C," *Solid State Ionics.*, 3-4, pp. 477-481.
- [14] Ranga Rao, G., and Ranjan Sahu, H., 2001, "XRD and UV-Vis diffuse reflectance analysis of  $CeO_2$ - $ZrO_2$  solid solutions synthesized by combustion method," *Proc. Indian Acad.Sci.(Chem.Sci.)*, Vol.113, Nov 5 & 6, Oct-Dec', pp. 651-658.
- [15] Gibson, I.R., Dransfield, G.P., and Irvine, J.T.S., 1998, "Influence of yttria concentration upon electrical properties and susceptibility to ageing of yttria-stabilised zirconias," *J. Eur. Ceram. Soc.*, 18, pp. 661-667.
- [16] XU Dapeng, WANG Quanyong, LU Zhe, LIU Zhiguo, ZHANG Gongmu., and SU Wenhui, May 2001, "High-pressure synthesis and properties of  $CeO_2$ - $ZrO_2$  solid solution," *Chinese Science Bulletin.*, Vol.46, No.10, pp.801-805.
- [17] Chiodelli, G, Flor, G., and Scagliotti, M, 1996, "Electrical properties of the  $ZrO_2$ - $CeO_2$  system," *Solid State Ionics.*, 91, pp. 109-121.
- [18] Bin Zhu, Xiaoguang Luo, Changring Xia, Albinsson, I., and Mellander, B.E., 1997, "Electrical properties of the  $ZrO_2$ - $CeO_2$  at Intermediate temperatures," *Ionics.*, 3, pp. 363-367.
- [19] Takahisa Omata, Yuji Goto, Shinya Otsuka-Yao-Matsuo., 2007, "Nanocrystals of zirconia and ceria-based solid electrolytes: Synthesis and properties," *Science and Technology of Advanced Materials.*, 8, pp. 524-530 and references cited in there.
- [20] Lee, J.H, Yoon, S.M, Kim, B.K, Lee, H.W., and Song. H.S., 2002, "The Electrical conductivity and defect structure of  $CeO_2$ - $ZrO_2$  mixed oxide," *Journal of Materials Science.*, 37, pp. 1165-1171.
- [21] Marta Boaro, Alessandro Trovarelli, Jin-Ha Hwang., and Thomas O. Mason, 2002, "Electrical and oxygen storage/release properties of nanocrystalline ceria-zirconia solid solutions," *Solid State Ionics.*, 147, pp. 85-95.

- [22] Dutta, P., and Biswas, S., 2002, "Dielectric relaxation in polyaniline-polyvinyl alcohol composites," *Mater. Res. Bull.*, 37, pp.193–200.
- [23] Indulal, C.R, Vaidyan, A.V., Sajeev Kumar, G., and Raveedran, R., 2010, "Characterization, dielectric and optical studies of nano-cerium phosphor iodate synthesized by chemical co-precipitation method," *Indian Journal of Engineering & Materials sciences*, 17, pp. 299-304.
- [24] Mo Chi-Mei., Zhang Lide., and Wang Guozhong., 1995, Characteristics of dielectric behavior in nanostructured materials, *Nanostructr. Mater*, 6, pp.823-826.
- [25] Maier, J., Prill, S., and Reichert, B., 1988, "Space charge effects in polycrystalline, micropolycrystalline and thin film samples: Application to AgCl and AgBr," *Solid State Ionics*, 28-30(2), pp.1465-1469.
- [26] Tareev, B., 1979, "Physics of dielectric Materials," Moscow Mir Publications, p. 107.
- [27] Kalai Selvan, R., Augustin, C.O., Sepelák, V., John Berchmans, L., Sanjeeviraja, C., and Gedanken, A., 2008, "Synthesis and characterization of CuFe<sub>2</sub>O<sub>4</sub>/CeO<sub>2</sub> nanocomposites," *Materials Chemistry and Physics*, 112, pp. 373-380.
- [28] Prabu, M., Selvasekarapandian, S., Kulkarni, A.R., Hirankumar, G., and Sanjeeviraja, C., 2010, "Conductivity and dielectric studies on LiCeO<sub>2</sub>," *Journal of rare earths*, 28 (3), pp. 435-438.